

Dust Studies in DIII-D and TEXTOR

D.L. Rudakov, J.H. Yu, J.A. Boedo, E.M. Hollmann, S.I. Krasheninnikov,
R.A. Moyer, A.Y. Pigarov, M. Rosenberg, R.D. Smirnov
University of California, San Diego

A.Litnovsky, S. Brezinsek, A. Huber, A. Kreter, V. Philipps, A. Pospieszczyk,
G. Sergienko

Institut für Energieforschung-Plasmaphysik, Forschungszentrum Jülich

W.P. West, B.D. Bray, N.H. Brooks, A.W. Hyatt, C.P.C. Wong
General Atomics

M. Groth, M.E. Fenstermacher, C.J. Lasnier
Lawrence Livermore National Laboratory

J.P. Sharpe
Idaho National Engineering and Environmental Laboratory

W.M. Solomon
Princeton Plasma Physics Laboratory

J.G. Watkins
Sandia National Laboratories





Second United Nations
International Conference
on the Peaceful Uses
of Atomic Energy

A/CONF.15/P/2214
USSR
8 August 1958

ENGLISH *
ORIGINAL: RUSSIAN

Confidential until official release during Conference

DYNAMICS OF RAREFIED PLASMA
IN A MAGNETIC FIELD

by R.S.Sagdeyev, B.B.Kadomtsev,
L.I.Rudakov and A.A.Vedyonov

The present paper deals with the properties of high-temperature plasma in a magnetic field. It has been shown that even in the absence of collisions, it is possible in a number of cases to describe plasma by using the hydrodynamic equations for compressible fluid with a non-isotropic pressure tensor.

The problem of equilibrium and stability of plasma with a pressure appreciably less than that of magnetic field was investigated by expanding the initial equations in a series of powers of a small parameter $\frac{8\pi P}{B^2}$. Instability of plasma with a non-isotropic velocity distribution in a magnetic field was also considered. It has been shown that the non-isotropy of temperature (parallel and perpendicular to the magnetic field) leads to a new type of instability. The criteria of such an instability

Motivation

Dust Presents Potential Problem in ITER

- ❖ Though dust is commonly found in fusion devices, in existing machines it is usually of little concern from either operational or safety standpoint
- ❖ **Dust generation in ITER is expected to increase by several orders of magnitude compared to existing machines**
- ❖ Dust accumulation can present a problem in ITER for a number of reasons:
 - C dust: Tritium retention
 - W dust: accumulation of radioactive material
 - Be dust: Hydrogen explosion hazard (in case of simultaneous water and air ingress)
- ❖ **Dust accumulation is a licensing issue in ITER with two separate limits:**
 - 1 tonne total in-vessel dust inventory
 - ~10 kg of Be and C dust on hot surfaces (above 400C)

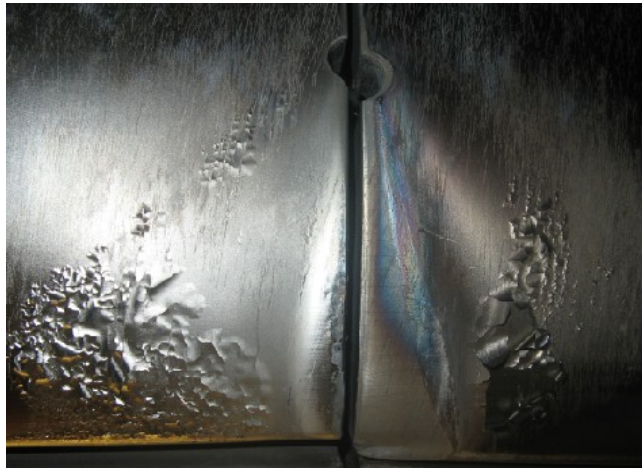
Projections of dust production and accumulation rates are needed

- ❖ **Dust may cause core contamination and degrade performance**

Studies of the dust transport and dynamics are important

**Observations of
naturally occurring and
unintentionally introduced
dust in DIII-D**

Sources of Naturally Occurring Dust in DIII-D



- Flakes from redeposited hydrocarbon films



- Monopolar arcs



- Thermal stress induced fracture



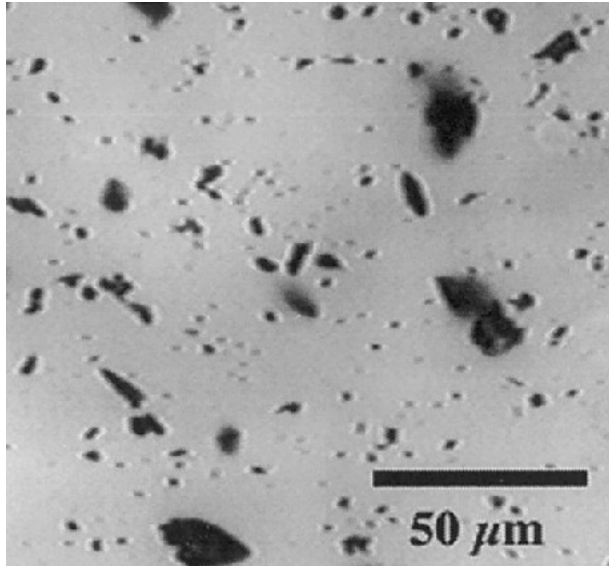
- Leading edges

Particles left from entry vent activities - *unintentionally introduced dust*

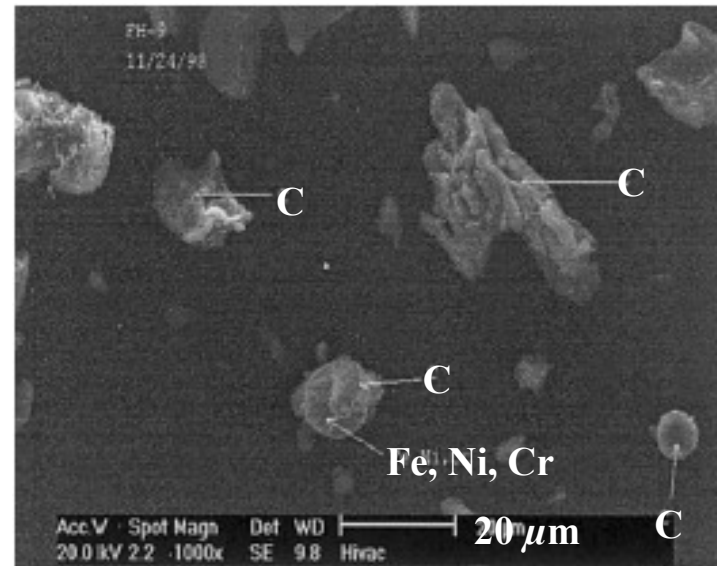
Dust Collected During Entry Vents

- ❖ Collection allows determination of dust size distribution, chemical composition, and estimation of the in-vessel dust inventory

W. J. Carmack, *et. al.*, Fusion Eng. Des. 51–52 (2000) 477



Optical microscope photograph
of DIII-D dust

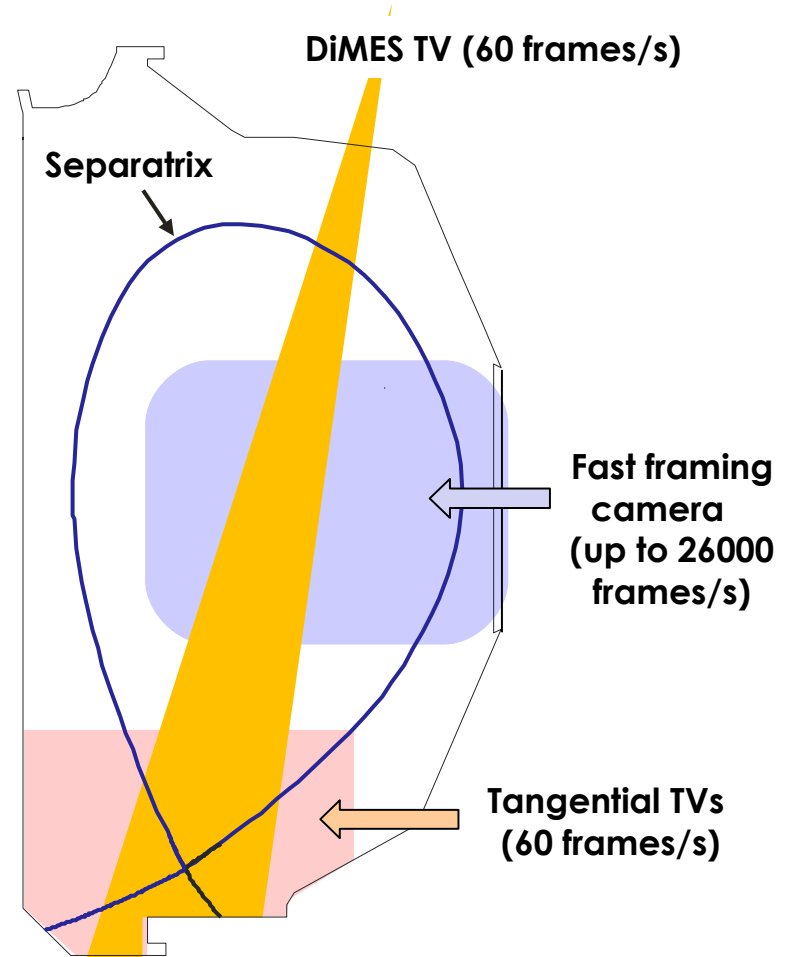
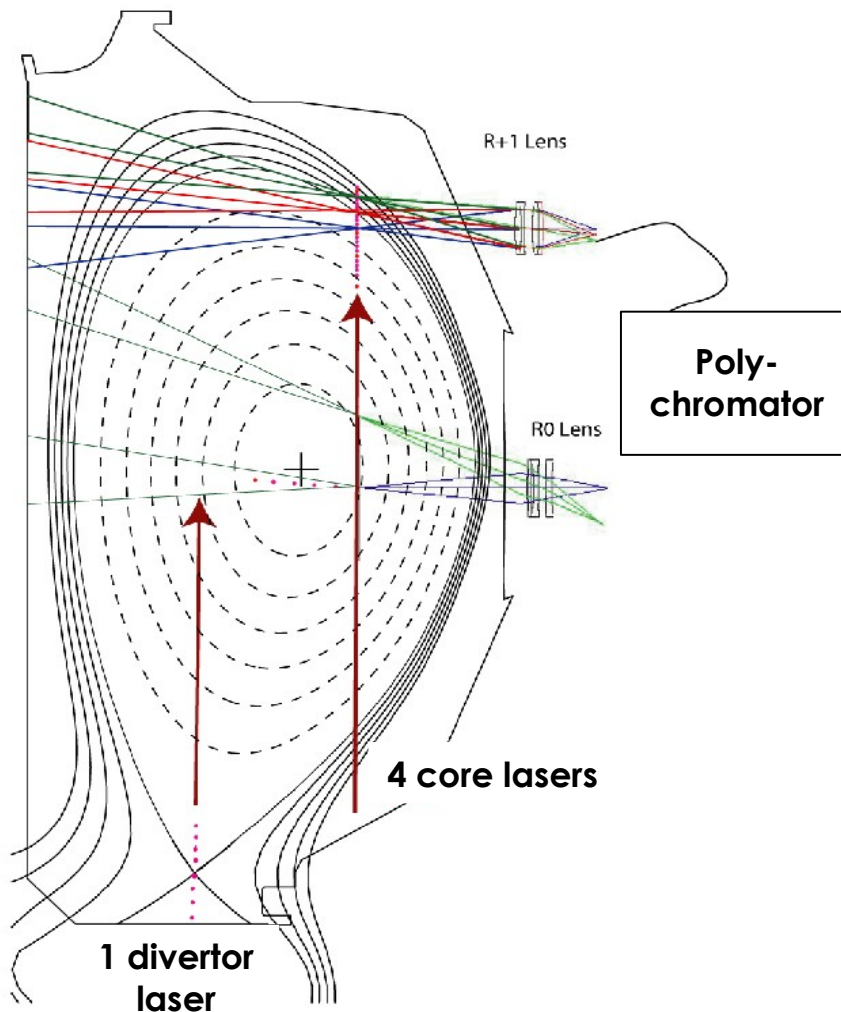


SEM photomicrograph of DIII-D dust

- ❖ Count median diameter: 0.46 – 1.0 μm (varied by sample)
- ❖ Chemical composition: mostly C with some impurities
- ❖ Amount of dust on divertor surfaces: ~ 1 g
- ❖ Estimated in-vessel inventory (including underneath tiles): ~ 30 g

Note: dust underneath tiles results mostly from graffoil compliant layers

Diagnostics of Dust in DIII-D Plasmas



❖ **Laser scattering** resolves particles
0.16 – 1.6 μm in diameter

❖ **Optical imaging** sensitive to larger particles

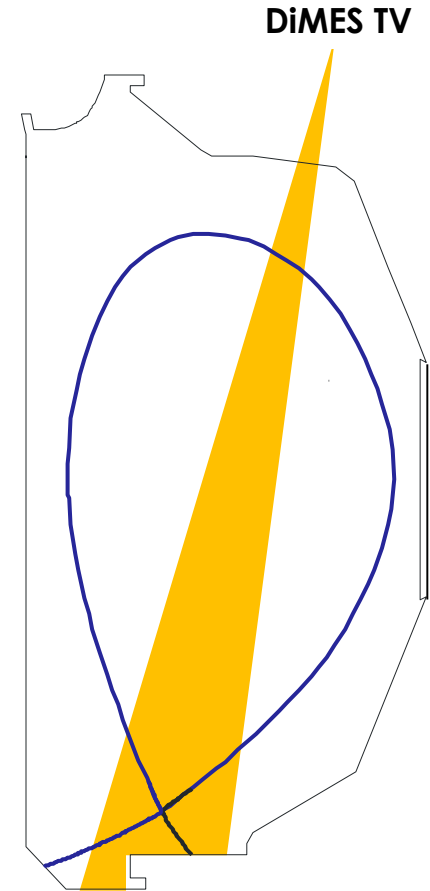
- ✓ ~4 μm and above (fast camera)
- ✓ tens of microns (standard rate cameras)

Dust Levels in DIII-D Are Normally Low, Elevated After an Entry Vent

- ❖ During “normal operations” (when the vacuum vessel walls are well conditioned and there are no major disruptions), dust observation rates in DIII-D are low: standard cameras register only isolated dust events, while the fast camera typically observes between 10-100 events per discharge
- ❖ **After an entry vent dust levels are elevated**
- ❖ In the first 2-3 plasma discharges after an entry vent dust levels are up to 100 times higher than during normal operations

Dust Observations Following an Entry Vent

Shot number 127331 – second plasma shot of 2007



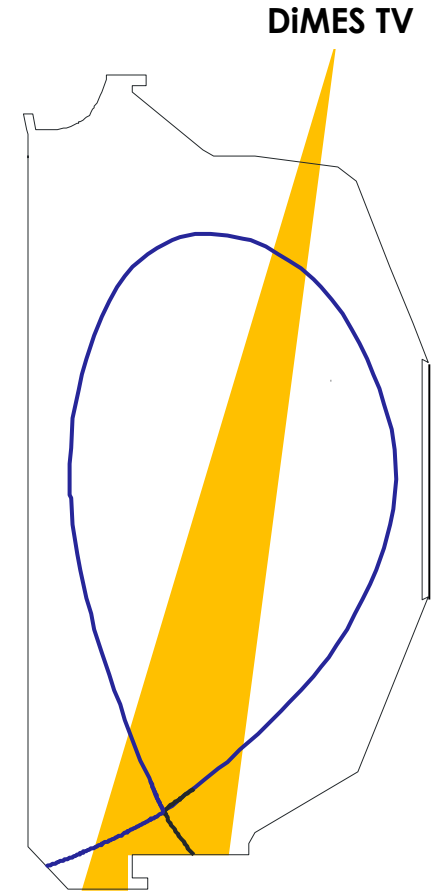
DiMES TV, looking down in lower divertor
near IR filter, 60 f/s, total duration ~3 s

Dust Levels in DIII-D Are Normally Low, Elevated After an Entry Vent

- ❖ During “normal operations” (when the vacuum vessel walls are well conditioned and there are no major disruptions), dust observation rates in DIII-D are low: standard cameras register only isolated dust events, while the fast camera typically observes between 10-100 events per discharge
- ❖ After an entry vent dust levels are elevated
- ❖ In the first 2-3 plasma discharges after an entry vent dust levels are up to 100 times higher than during normal operations
- ❖ After ~10 plasma discharges dust was observed mostly at the beginning and end of each discharge

Dust Observations Following an Entry Vent

Shot number 127341 – 12th plasma shot of 2007



DiMES TV, looking down in lower divertor
near IR filter, 60 f/s, total duration ~3 s

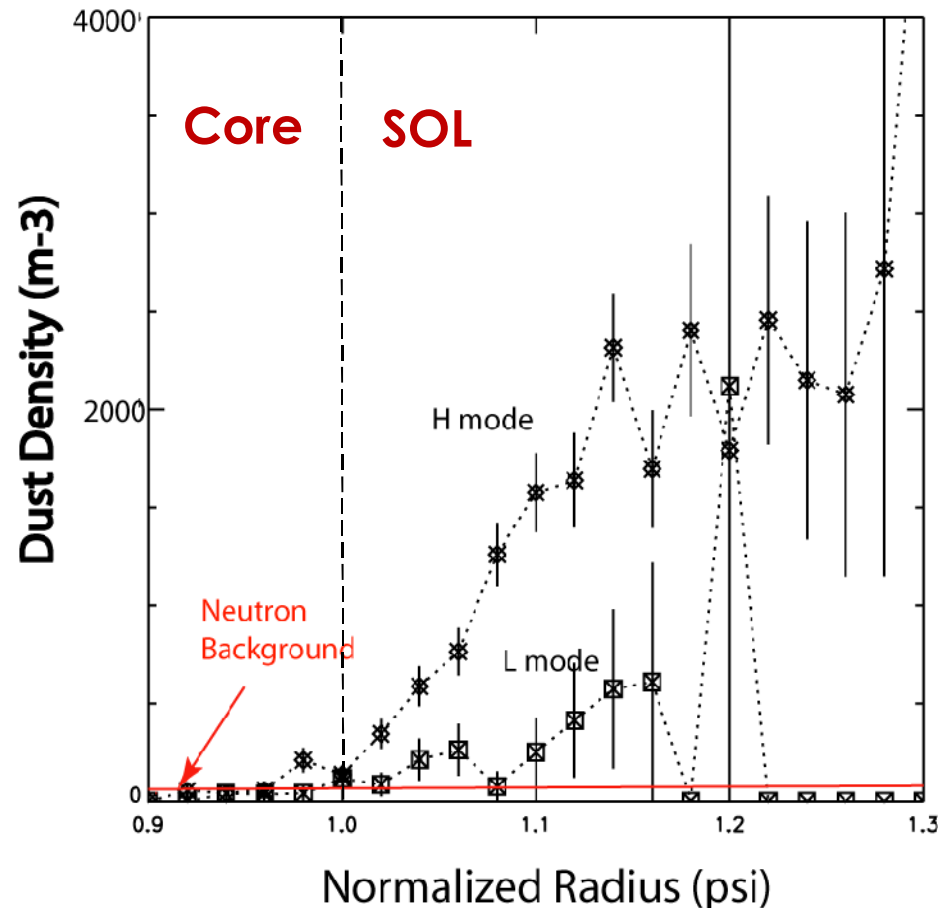
Dust Levels in DIII-D Are Normally Low, Elevated After an Entry Vent

- ❖ During “normal operations” (when the vacuum vessel walls are well conditioned and there are no major disruptions), dust observation rates in DIII-D are low: standard cameras register only isolated dust events, while the fast camera typically observes between 10-100 events per discharge
- ❖ After an entry vent dust levels are elevated
- ❖ In the first 2-3 plasma discharges after 2006-07 entry vent dust levels were up to 100 times higher than during normal operations
- ❖ After ~10 plasma discharges dust was observed mostly at the beginning and end of each discharge
- ❖ After ~70 plasma discharges dust levels are reduced to normal

Plasma contact removes loose dust from PFC surfaces

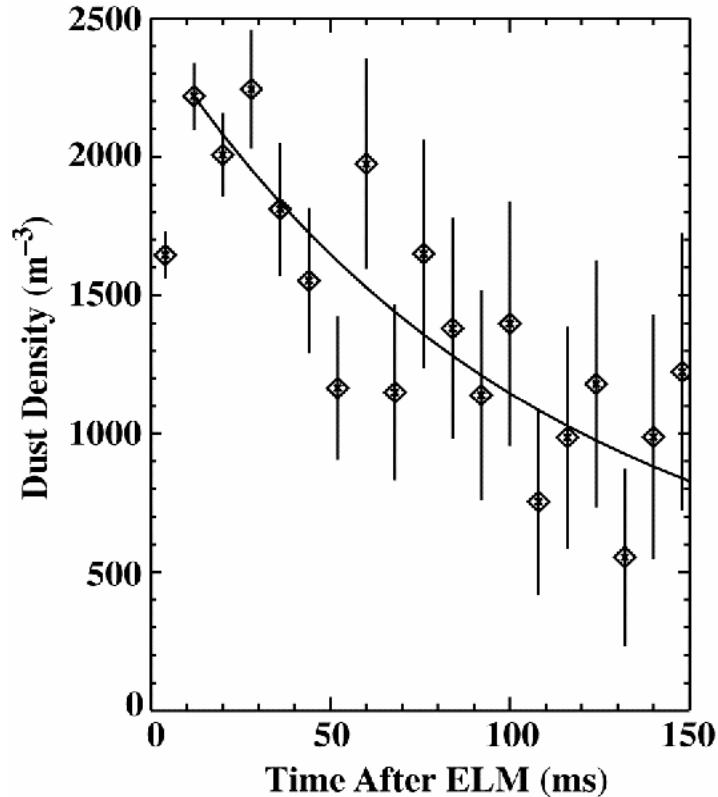
Dust Density Increases from LCFS into SOL

- ❖ During “normal operations”, statistical average of the dust density can be estimated from the laser scattering event rate
- ❖ The dust density is at or below the detection limit in the core plasma and increases with distance into the scrape-off layer (SOL)
- ❖ H-mode discharges with ELMs have significantly higher dust densities than L-mode discharges

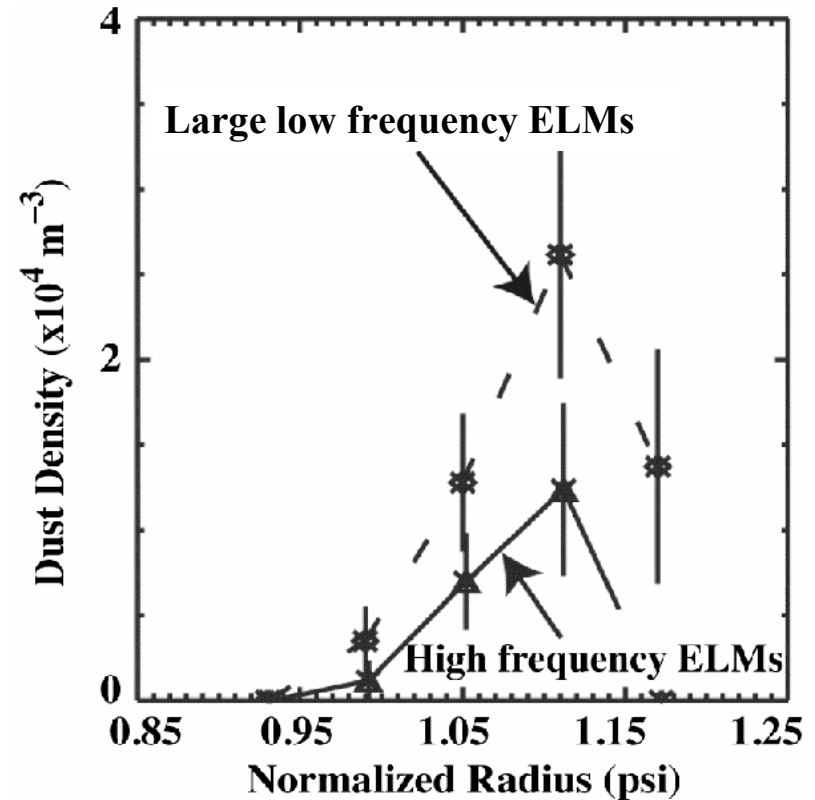


Dust Observation Rates Correlate with ELMs

- ❖ Statistical analysis of the laser scattering data shows that dust observation rates are higher immediately after an ELM



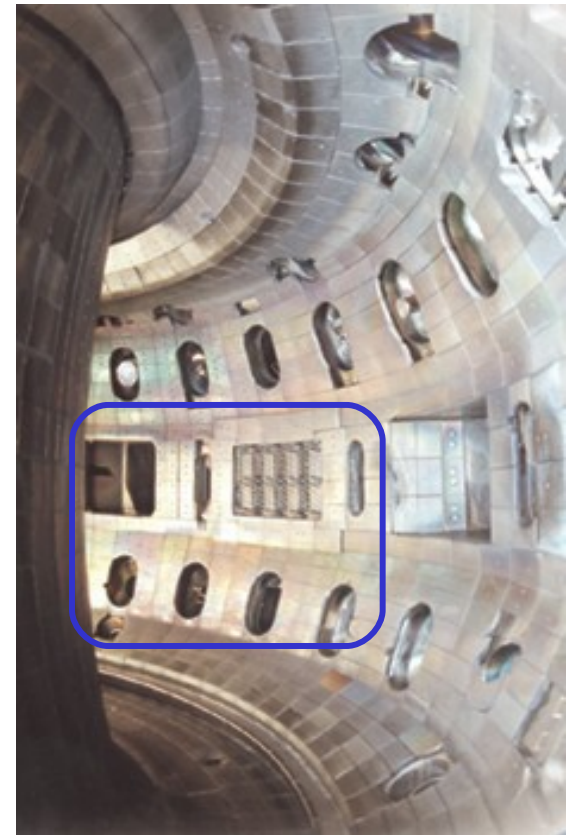
- ❖ Average dust density decreases with time after an ELM



- ❖ Large low frequency ELMs result in more dust than small high frequency ELMs

Direct Observation of Dust Release after an ELM

Shot number 132476



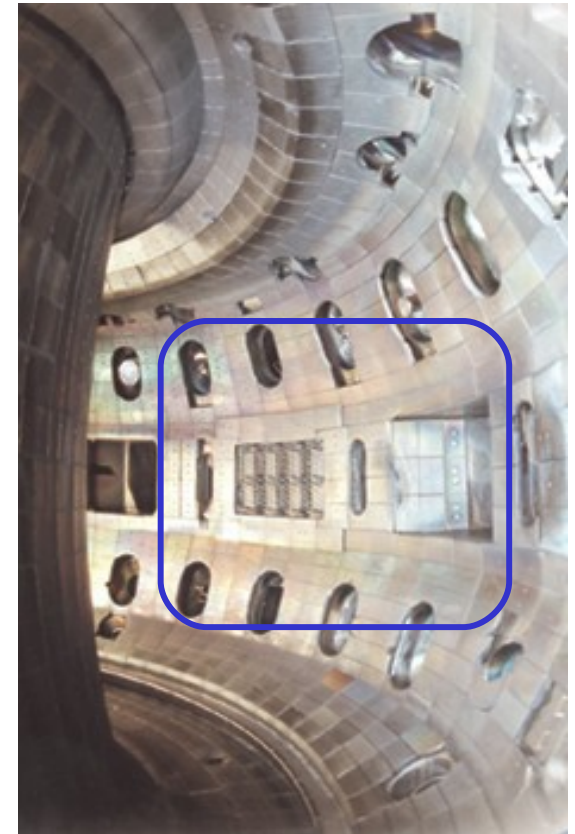
Full light, 26000 f/s, total duration ~ 3 ms

Disruptions Result in Dust Release

- ❖ **Statistical analysis of scattering data shows that discharges following disruptions have higher dust density**
- ❖ **Sometimes fast camera sees a “dust shower” following a disruption**

Disruptions Result in Dust Release

Shot number 131255, upward VDE



Full light, 4000 f/s, total duration ~ 50 ms

Disruptions Result in Dust Release

- ❖ Statistical analysis of scattering data shows that discharges following disruptions have higher dust density
- ❖ Sometimes fast camera sees a “dust shower” following a disruption
- ❖ Post-disruption dust velocities are rather high (up to 100s m/s) and directions of motion are not consistent with dust release by mechanical shaking of the vessel
- ❖ **Dust is most likely released at the areas of most intense plasma-wall contact**
- ❖ Whether disruptions actually produce dust or just blow off dust accumulated on the PFC surfaces remains an open question

Estimated Dust Formation Rates in DIII-D are MUCH Lower Than the Net Erosion Rate of Divertor Targets

- ❖ Over a campaign with 1400 lower single null discharges, total net erosion near the outer strike point (OSP) measured by profilometry was ~22 g of C [C. Wong et al., JNM 196-198 (1992) 871]
- ❖ 78% of eroded C was found in re-deposited films near the inner strike point
- ❖ Independent estimate using net erosion rate of 3 nm/s measured at the OSP in H-mode with Divertor Material Evaluation System (DiMES) gives a similar result for 1400 5-second discharges: ~18 g of net C erosion at OSP
- ❖ From the scattering data, total amount of sub-micron dust per campaign is ~1 g; most of this dust is probably ablated in the plasma
- ❖ Total amount of dust released by disruptions per campaign estimated from the fast camera data is <1 g

Most of eroded carbon in DIII-D does not end up as mobilizable dust

Properties of the naturally occurring dust in DIII-D

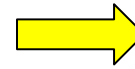
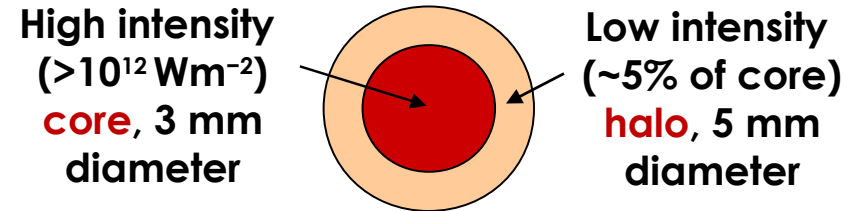
Submicron dust size Can Be Estimated From the Amplitude of the Scattered Signal

- An analysis using a Mie scattering model and taking into account particle ablation by the laser has put the resolvable particle size within the range of $0.16\text{--}1.6\ \mu\text{m}$ in diameter

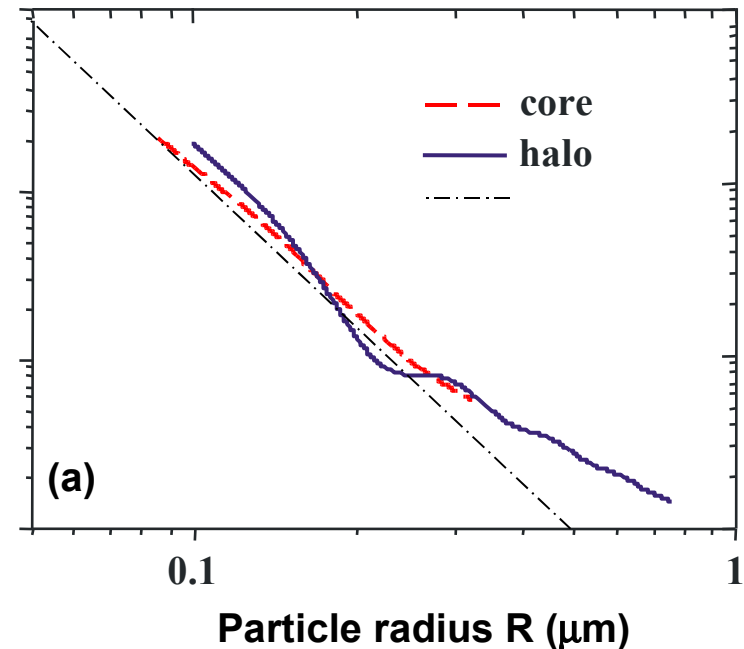
R.D. Smirnov, et. al., PoP 14 (2007) 112507

- The total carbon content of the dust is less than a few percent of the total carbon content of the plasma

Laser beam structure

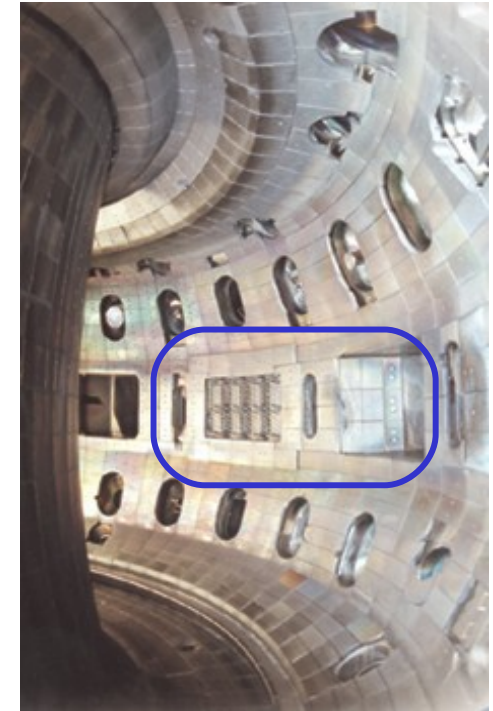


PDF (a.u.)



Characteristics of the dust observed by cameras

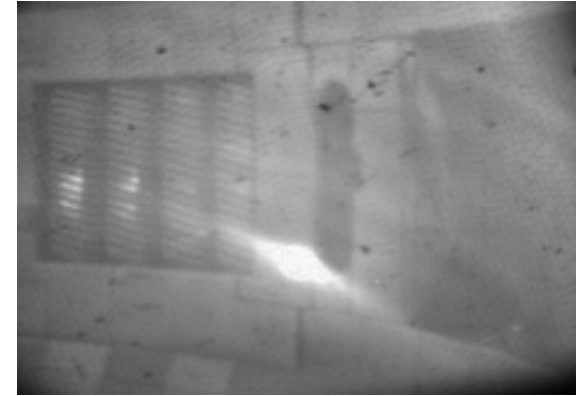
- ❖ Velocities from a few m/s up to ~ 300 m/s
- ❖ Sometimes breakup of large particles into pieces is observed
- ❖ Some particles develop ablation clouds stretched along B-field



Full light, 2000 f/s, total duration ~100 ms

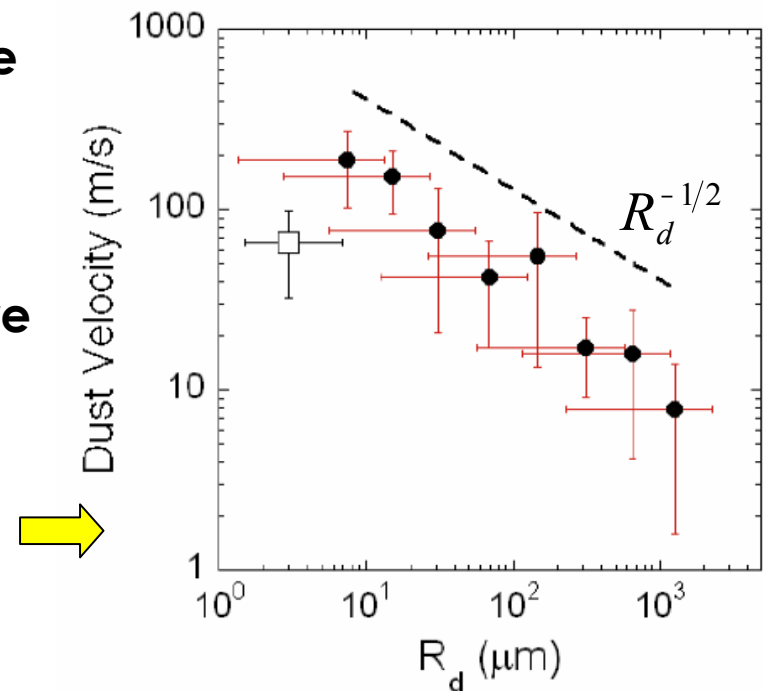
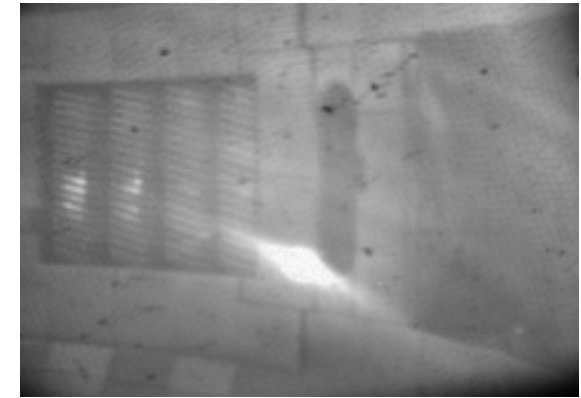
Determination of the Particle Size From Camera Data is Difficult

- ❖ It's hardly possible to determine the particle size from the image brightness because
 - a) plasma parameters at the particle location are not exactly known
 - b) line radiation from the ablation cloud often dominates the detected radiation



Determination of the Particle Size From Camera Data is Difficult **but Not Impossible**

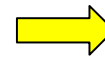
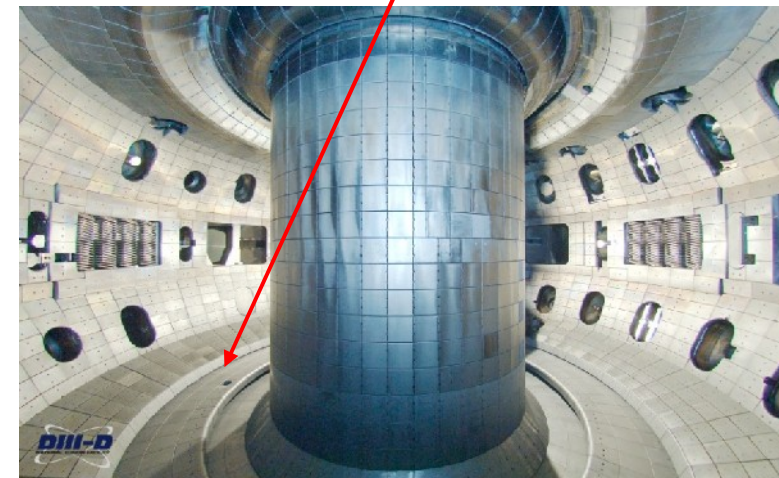
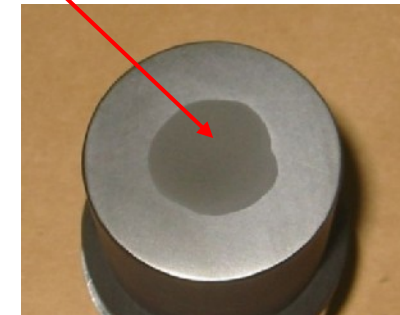
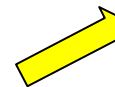
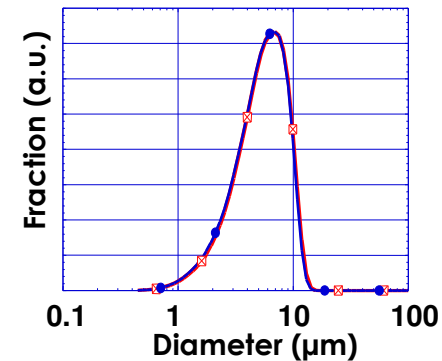
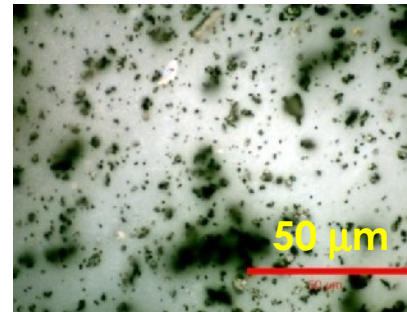
- ❖ It's hardly possible to determine the particle size from the image brightness because
 - plasma parameters at the particle location are not exactly known
 - line radiation from the ablation cloud often dominates the detected radiation
- ❖ An alternative approach involves comparison of a particle life time in the plasma with a theoretical ablation rate of a carbon sphere
- ❖ **This method has been recently applied to DIII-D data with encouraging results**
- ❖ Particle sizes between $6\ \mu\text{m}$ and $\sim 1\text{mm}$ were inferred
- ❖ Inverse dependence of the 2D velocity on size with a slope $\sim R_d^{-1/2}$ was found



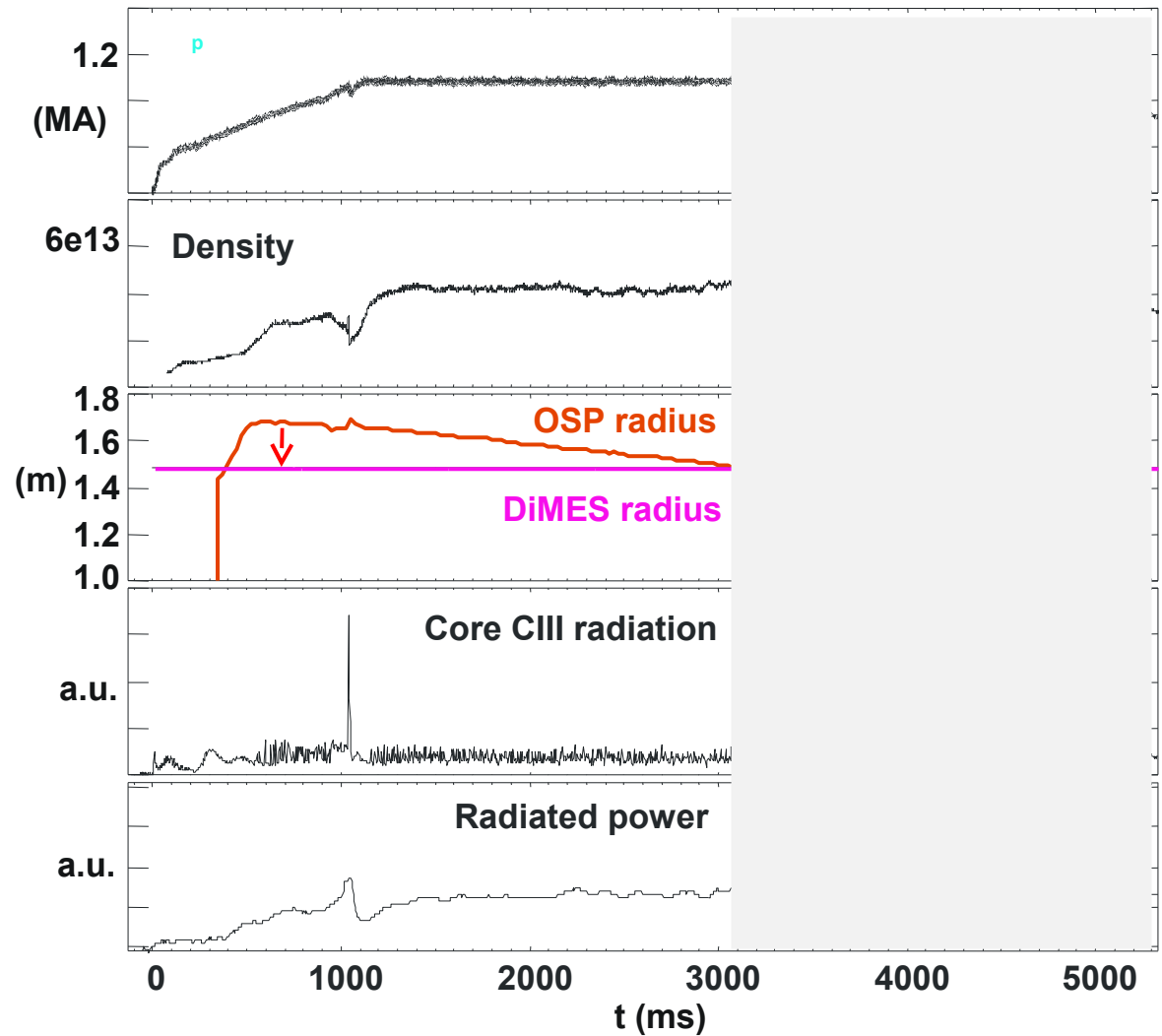
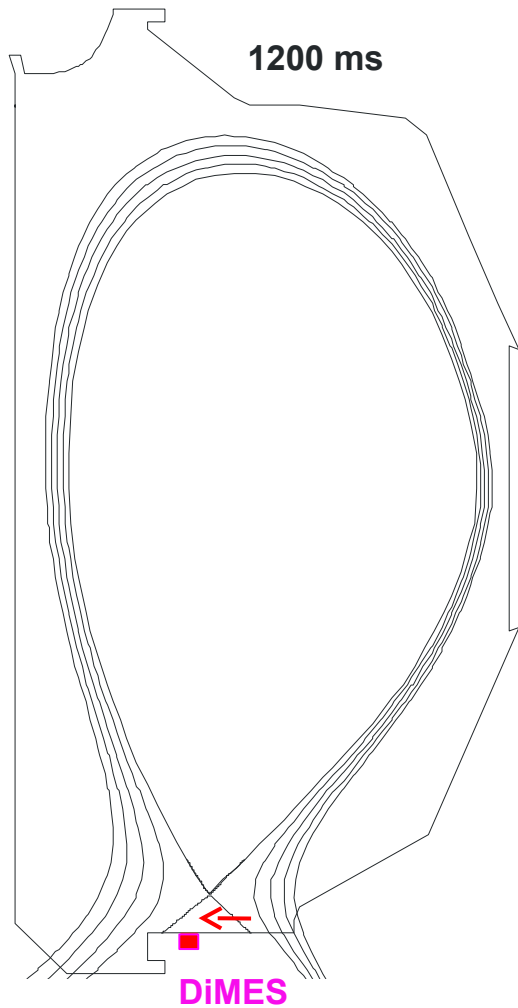
Experiments with
intentionally introduced
carbon dust
in DIII-D and TEXTOR

Motivation for Dust Injection and Technique Used

- ❖ The aims of the dust injection:
 - ✓ Calibrate diagnostics
 - ✓ Benchmark *DustT* code modeling of dust dynamics
- ❖ Graphite dust with tokamak-relevant size (median diameter of $6\ \mu\text{m}$) obtained from Toyo Tanso Company, Ltd.
- ❖ Suspension of $\sim 30\text{-}40\ \text{mg}$ of dust in ethanol loaded in a graphite holder and allowed to dry
- ❖ Holder with dust inserted in the lower divertor of DIII-D using Divertor Material Evaluation System (DiMES) manipulator

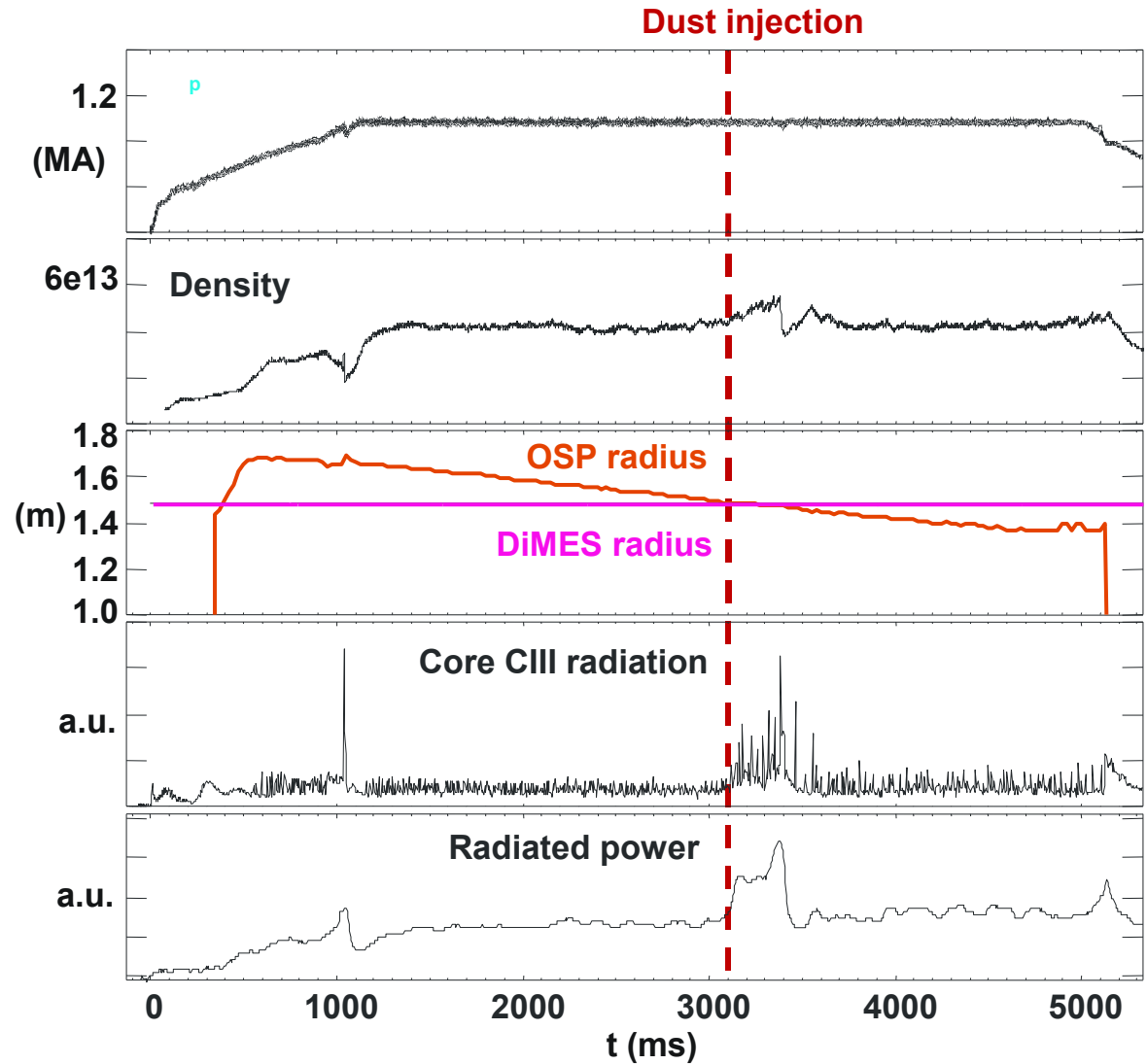


Dust Exposed to LSN H-mode with Swept Strike Points



- Between 0.5-3 sec DiMES is located in the private flux region
- Outer strike point (OSP) is slowly swept towards DiMES

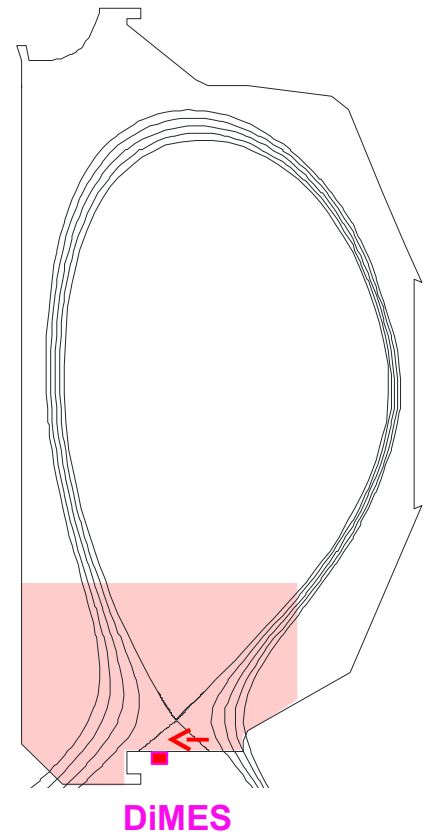
Dust Exposed to LSN H-mode with Swept Strike Points



- When OSP reaches DiMES, a massive dust injection occurs
- Core CIII light and radiated power double after the injection

Dust Injection from DiMES Observed Directly

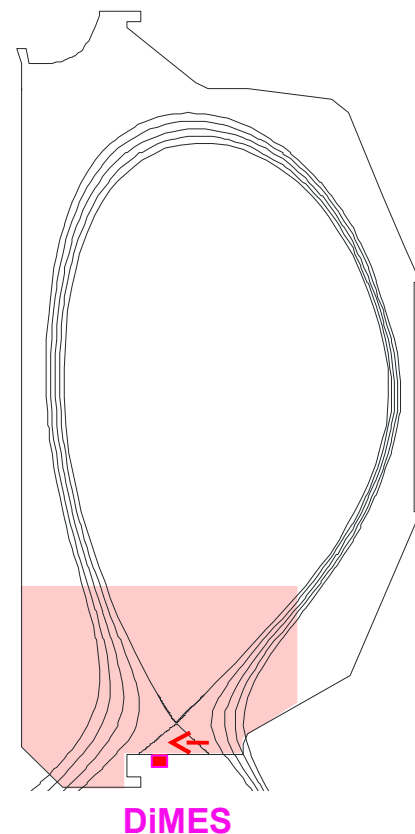
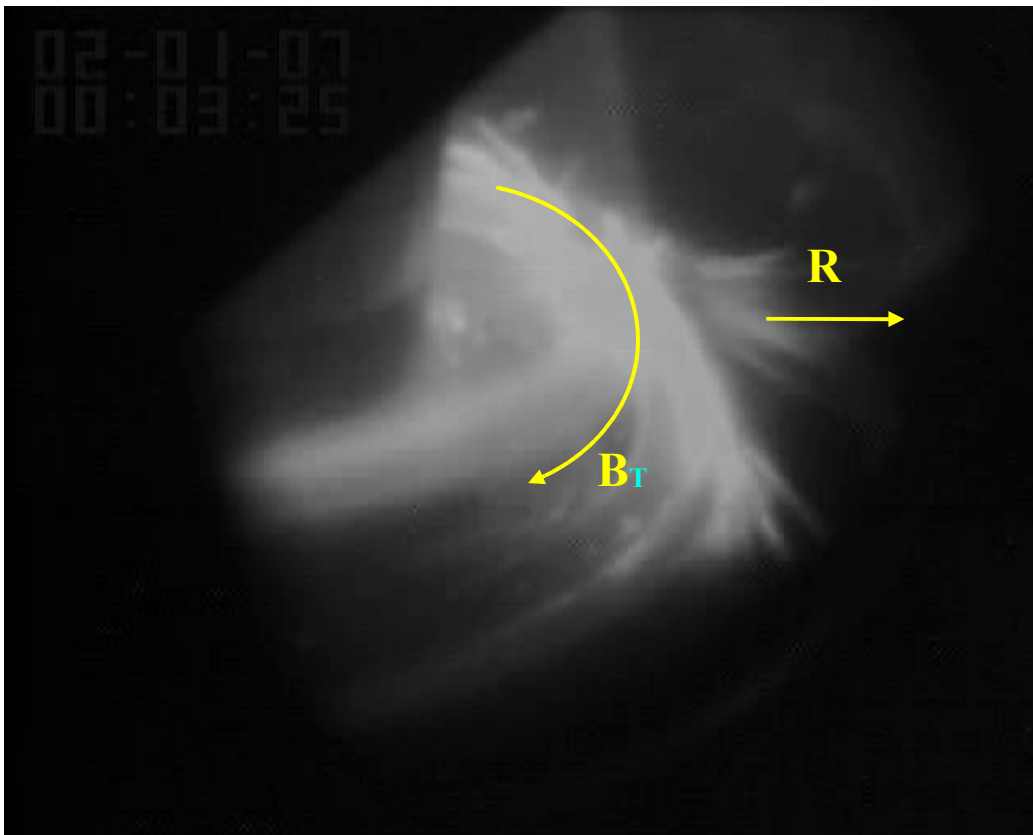
Shot number 127641



Tangential TV, near IR filter, 60 f/s

Dust Motion is Mostly in the Toroidal Direction

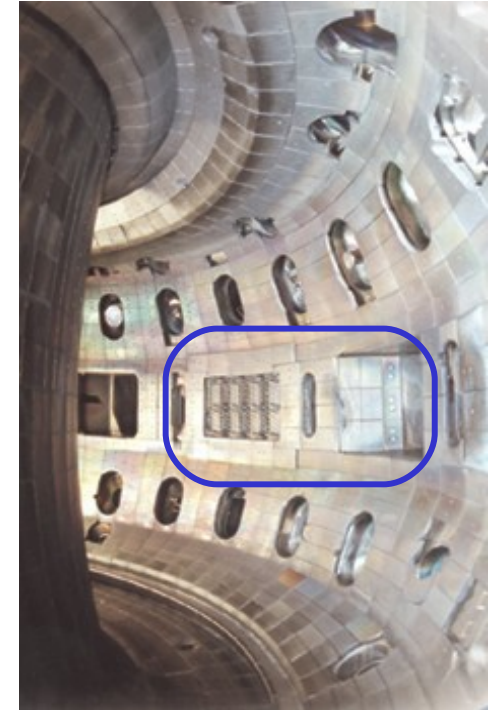
Shot number 127641



Tangential TV, near IR filter, 60 f/s

Dust Injected from DiMES Observed in Outboard SOL

Shot number 127641



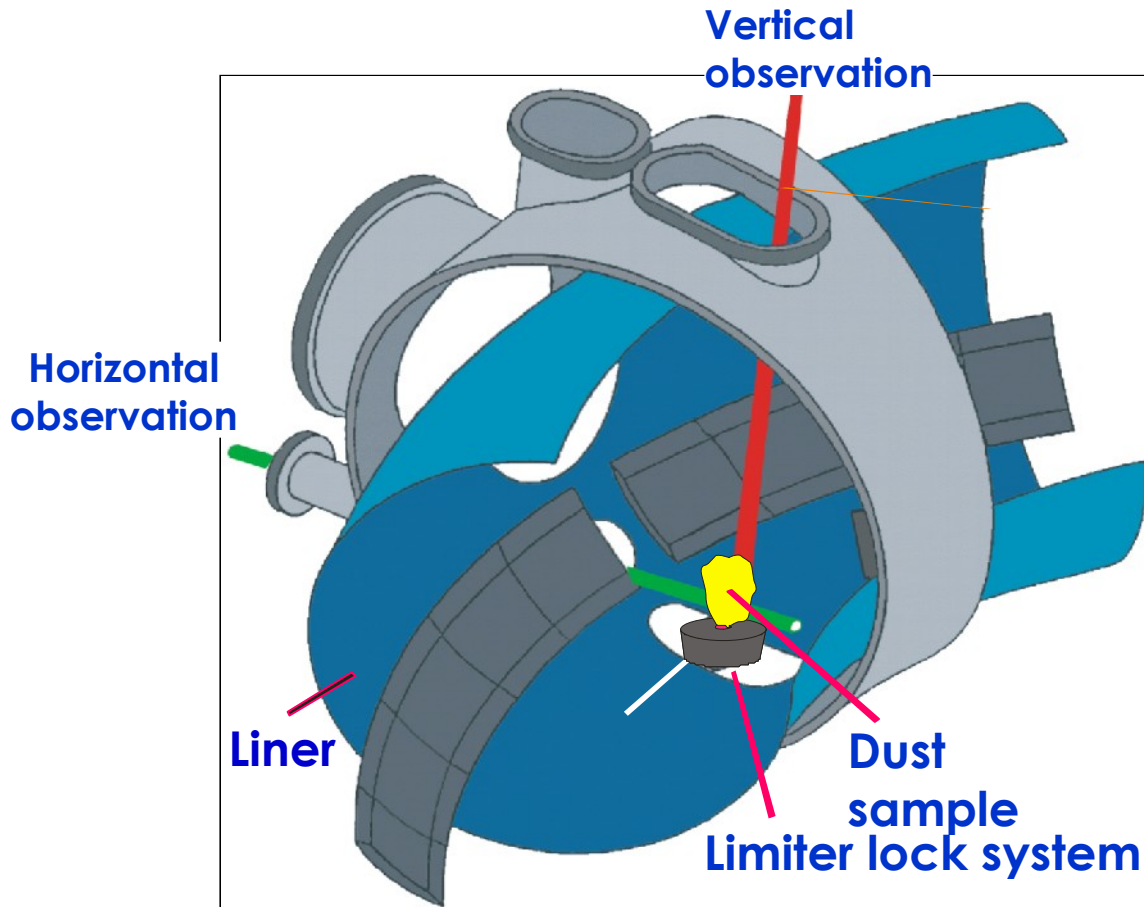
DiMES

Full light, 3000 f/s, total duration ~ 1 s
Bright flashes of light are due to ELMS

Dust Injection Experiment on TEXTOR

- Aims:**
- Investigations of an impact of dust on core and edge plasmas
 - Search for possible TEXTOR - DIII-D similarities

Used the same graphite dust as in DIII-D experiment



Dust holder insert

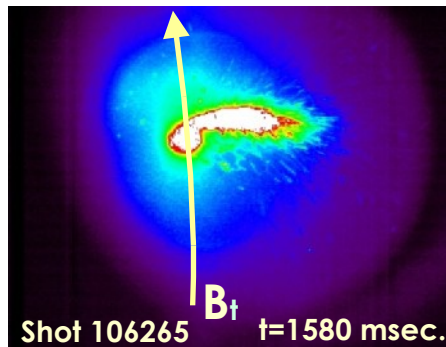


Limiter head

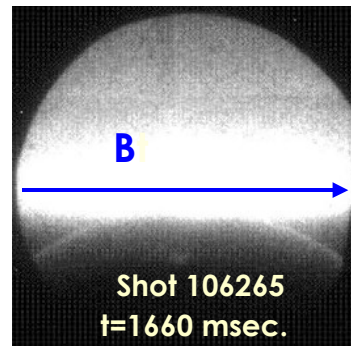
Limiter with dust



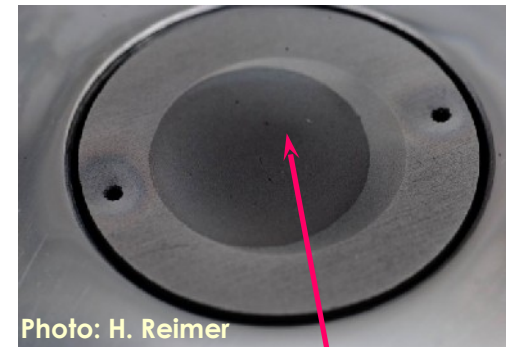
- ❖ Dust exposed to discharges heated with 1.4 MW of neutral beam injection
- ❖ Limiter exposed at different radial distances to check launch efficiency
- ❖ 3 dust inserts tested with different amount of dust: from 1 to 45 mg
- ❖ Maximum amount of dust launched: ~ 40 mg ($\sim 2 \times 10^{21}$ C atoms)



Dust launch, view of the limiter by the vertical camera (no filter)



Dust launch, view of the limiter by the horizontal camera (CIII filter)



Remaining dust "baked" with the holder after exposure

- ❖ Dust was launched either in the beginning of a discharge or at $t=1.5$ s, when the neutral beam injection started
- ❖ Dust was moving perpendicularly to B_T , consistent with being launched by the Lorentz force due to the thermoelectron current emitted by the hot dust particles

- ❖ No measurable effect on Z_{eff}
- ❖ No increase of core carbon concentration (CV, CVI)

 **No effect on the core performance**

- ❖ Carbon concentration in the edge rose from ~3% to ~6%, implying that around 0.01% of launched dust carbon content entered the edge plasmas

 **Under the given conditions, most of the dust was deposited locally on the nearby plasma facing components without entering the core plasmas**

Comparison with modeling

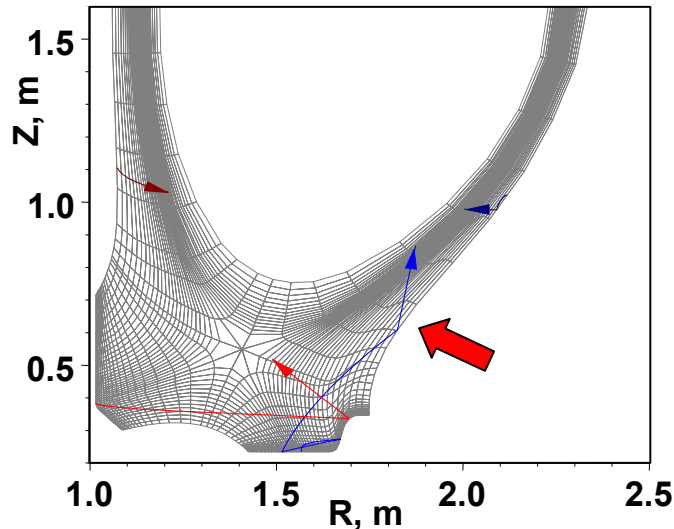
Dust Transport *DustT* code developed at UCSD

- ❖ *DustT* code solves equations of motion (r,v) for dust particle self-consistently in 3D
- ❖ The code uses magnetic equilibrium mesh and plasma background from UEDGE code
- ❖ Based on UEDGE data, the forces acting on dust particle from plasma are calculated
- ❖ *DustT* employs Monte Carlo method for incorporating the dust collisions with walls and micro-turbulence
- ❖ Dust of different chemical compositions can be modeled

DIII-D Experimental results are in agreement with *DustT*

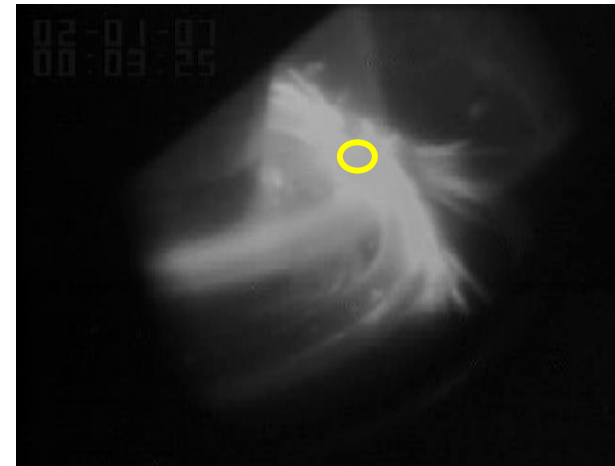
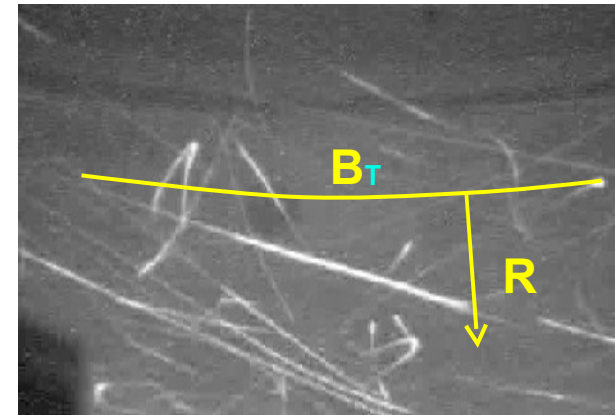
DustT

- Velocity of dust in plasma $\sim 1-100$ s m/s
- Dust particles are accelerated in the direction of plasma flow
- Dust trajectories are “elongated” in the toroidal direction
- Micron size dust launched in the lower divertor can reach mid-plane



Experiment

Dust velocities $\sim 3-300$ m/s



Modeling of TEXTOR experiment is forthcoming

SUMMARY

- ❖ ELMs and disruptions result in dust release in DIII-D
- ❖ Plasma contact tends to remove dust from PFC surfaces
- ❖ Most of carbon eroded from DIII-D divertor does not end up as mobilizable dust
- ❖ Micron-size carbon dust introduced in the lower divertor of DIII-D becomes highly mobile and results in core contamination
- ❖ Similar dust introduced in the SOL of TEXTOR did not penetrate the core plasma and moderately perturbed the edge plasma
- ❖ Modeling by *DustT* code is capable of reproducing experimentally observed dust velocities and trajectory shapes in DIII-D